JACS
JOURNAL OF THE AMERICAN CHEMICAL SOCIETY

COMMUNICATION

pubs.acs.org/JACS

Localized Surface Plasmon Resonances of Anisotropic Semiconductor Nanocrystals

Su-Wen Hsu, Kathy On, and Andrea R. Tao*

Department of NanoEngineering, University of California, San Diego, 9500 Gilman Drive, MC 0448, La Jolla, California 92039-0448, United States

Supporting Information

ABSTRACT: We demonstrate that anisotropic semiconductor nanocrystals display localized surface plasmon resonances that are dependent on the nanocrystal shape and cover a broad spectral region in the near-IR wavelengths. In-plane and out-of-plane dipolar resonances were observed for colloidal dispersions of $Cu_{2-x}S$ nanodisks, and the wavelengths of these resonances are in good agreement with calculations carried out in the electrostatic limit. The wavelength, line shape, and relative intensities of these plasmon bands can be tuned during the synthetic process by controlling the geometric aspect ratio of the disk or using a postsynthetic thermal-processing step to increase the free carrier densities.

Localized surface plasmon resonances (LSPRs) have been extensively characterized for metal nanoparticles that possess different sizes and shapes. While spherical metal nanoparticles typically possess a single dipolar LSPR, nanoparticles with anisotropic shapes, such as rods, cubes, disks, and triangular plates, have been demonstrated to exhibit multiple higher-order LSPR modes.[1−4] These LSPRs arise from the uneven charge distribution within the nonspherical particle volume and often result in large electromagnetic field enhancements localized near the corners and edges of the nanoparticles.[5,6] Because of this field enhancement, anisotropic nanoparticles composed of Ag and Au are currently being pursued as platforms for subwavelength focusing and imaging, surface-enhanced Raman spectroscopy, and photovoltaics.[7−9] More recently, LSPRs have been reported for nonmetallic nanocrystals composed of doped semiconductor materials such as $Cu_{2-x}S$, $Cu_{2-x}Se$, and most recently, Sb-doped SnO_2.[10−13] Plasmonic nanocrystals composed of these materials are advantageous because the LSPR wavelength can be dynamically tuned by controlling the free carrier density. This has been carried out through chemical and electrochemical doping processes. To date, the majority of work on plasmonic semiconductor nanocrystals has focused on characterizing *size-dependent* LSPRs for spherical nanocrystals.

Here we report for the first time the observation of *shape-dependent* LSPRs for $Cu_{2-x}S$ nanodisks that possess in-plane and out-of-plane dipoles associated with the ultrathin disk geometry. Previously, it was shown that $Cu_{2-x}S$ nanocrystals possess an LSPR mode in the near-IR (NIR) range whose wavelength can be tuned by introducing Cu vacancies into the $Cu_{2-x}S$ lattice.[10,13] Hole carriers generated by these vacancies are produced upon exposure of the nanocrystal to oxygen, which causes the LSPR band to blue-shift as the dopant concentration is increased. We have observed that nanodisks possess two distinct LSPR modes, as characterized by NIR transmission measurements. We demonstrate that these LSPR modes can be modulated by varying the aspect ratio of the disk. We also demonstrate that unlike the LSPR modes of Ag and Au nanoparticles, the LSPR modes of the $Cu_{2-x}S$ nanodisks can also be modulated by the dopant concentration.

To prepare the nanodisks, we used a solventless synthesis modified from previously published protocols.[14,15] A copper thiolate-derived precursor, $Cu(SCH_{12}H_{25})_2$, was prepared by mixing solutions of 1-dodecanethiol (4.83 mL, 20 mM) in ethanol and copper nitrate (1.16 g, 5 mM) in water. The resulting yellow-white precursor was separated and purified by centrifugation in ethanol and deionized water and then placed under vacuum to obtain a powder. This powder was heated at 200−220 °C to form a dark-brown solid composed of the $Cu_{2-x}S$ nanodisks. The dark-brown solid was redispersed in chloroform to remove any byproducts. The purified product was dried in a desiccator prior to characterization by X-ray diffraction (XRD), electron microscopy, and NIR transmission spectroscopy (Shimadzu UV3600). XRD indicated that the nanodisks possess a crystal symmetry that is closely related to the hexagonal lattice of chalcocite (Cu_2S) [see the Supporting Information (SI)]. Together with absorbance data, this result indicates that the nanodisks are most likely composed of djurleite with a stoichiometry close to $Cu_{1.96}S$. These nanodisks are oriented in such a way that the basal plane corresponds to the (002) plane and disk growth occurs orthogonal to the *c* axis in the ⟨110⟩ direction.[15] The size, shape, and Cu:S stoichiometry of the nanodisks can be controlled by tuning synthetic parameters such as the reaction temperature and time.

Figure 1 shows the NIR extinction spectra for colloidal dispersions of spherical $Cu_{2-x}S$ nanocrystals with a diameter of 4.0 ± 0.5 nm and flat $Cu_{2-x}S$ nanodisks with a basal-plane diameter of 24.5 ± 8.6 nm and a height of 4.4 ± 1.0 nm. The nanocrystals and nanodisks were dispersed in CCl_4 to minimize the spectral background resulting from solvent absorption. The corresponding transmission electron microscopy (TEM) images show nanocrystals obtained from a dried droplet of the colloidal dispersions. Upon solvent evaporation, the nanodisks undergo preferential assembly into stacks (as a result of hydrophobic interactions from dodecanethiol capping ligands) and appear

Received: September 28, 2011
Published: November 01, 2011

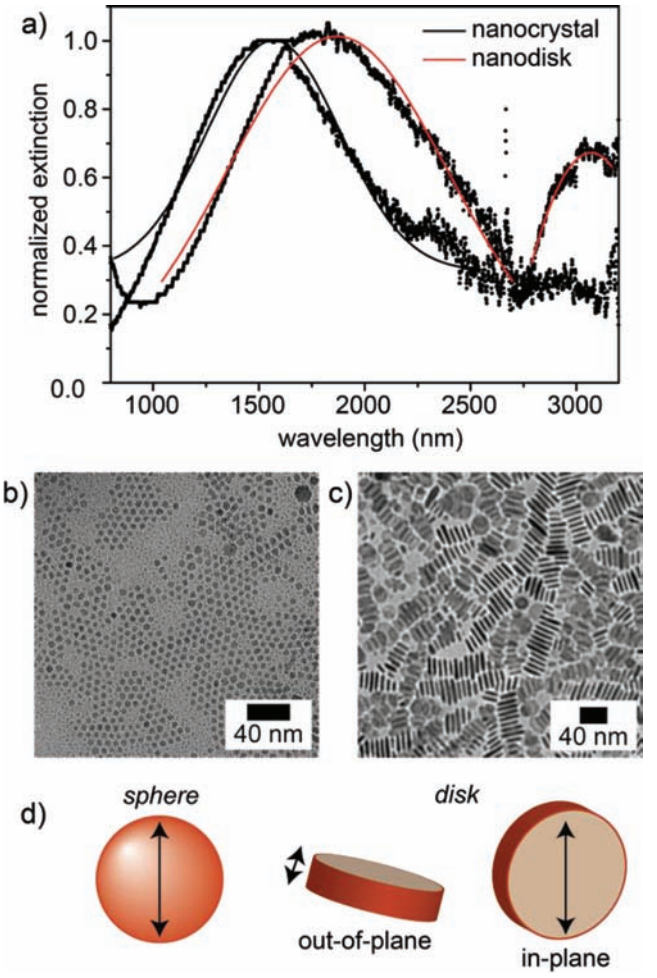

Figure 1. Shape-dependent LSPRs of $Cu_{2-x}S$ nanocrystals. (a) NIR extinction spectra (black dots) for colloidal dispersions of spherical nanocrystals and nanodisks. The black and red solid lines are the respective best fits of the extinction peaks, which were used to calculate the free carrier concentrations. (b) TEM image of spherical nanocrystals. (c) TEM image of nanodisks. (d) Schematic of LSPR polarizations for spherical and disk-shaped nanocrystals.

rodlike in the TEM image. The NIR spectrum of the nanodisk is characterized by two extinction bands near 1800 and 3100 nm. The presence of multiple extinction peaks is attributed to the excitation of shape-dependent dipolar LSPR modes, where excitation occurs for incident radiation polarized in two directions: parallel and perpendicular to the basal plane of the disk. In contrast, the dispersion of spherical nanocrystals gives rise to a single dipolar LSPR band near 1600 nm, consistent with previous reports that characterized $Cu_{2-x}S$ nanocrystals in a similar diameter range.[13] The onset of excitonic absorption for $Cu_{2-x}S$ nanocrystals occurs near 800 nm (depending on the Cu:S ratio and nanocrystal size) and does not show significant overlap with the spectral range shown here.

The LSPR wavelength depends on the complex dielectric function of $Cu_{2-x}S$ (ε), the dielectric function of the surrounding medium (ε_m), and the nanodisk size and shape. In the electrostatic limit, where $d \ll \lambda$, the dipole polarizability (α) of a nanodisk can be approximated using basic scattering theory for an oblate spheroid with semiaxes $a < b = c$.[16] The following

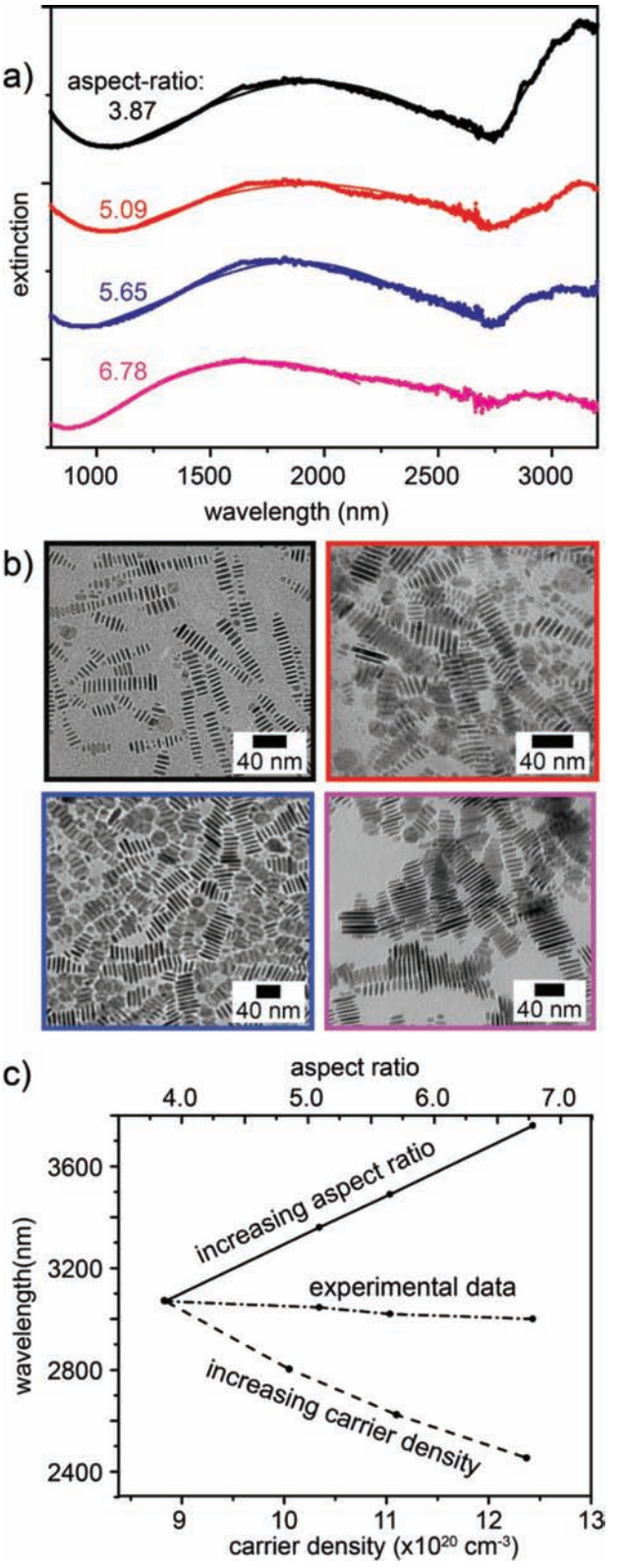

Figure 2. Change in LSPR properties with varying disk aspect ratio. (a) NIR extinction spectra of colloidal $Cu_{2-x}S$ nanodisk dispersions with aspect ratios as shown. (b) Corresponding TEM images of the nanodisk samples in (a). (c) Calculated change in LSPR wavelength for the in-plane mode for nanodisks with independently increasing aspect ratios (solid) and carrier densities (dashed), compared with the experimental data (dot-dash) obtained from the spectra in (a).

dx.doi.org/10.1021/ja2089876 |J. Am. Chem. Soc. 2011, 133, 19072–19075

expression is obtained:

$$\alpha_j = 3\varepsilon_0 V \frac{(\varepsilon - \varepsilon_m)}{3\varepsilon_m + 3L_j(\varepsilon - \varepsilon_m)}$$

where $j = 1, 2,$ or 3, V is the spheroid volume, ε_0 is the permittivity of free space, and L_j is a shape-dependent constant calculated from the spheroid axis lengths. For a disklike spheroid with an aspect ratio (diameter-to-height ratio) of 5, $L_1 = 0.588$ for the electric field perpendicular to the basal plane and $L_2 = L_3 = 0.206$ for the in-plane electric field. The resonance requirement is met for α_1 when

$$\varepsilon_r = -0.70\varepsilon_m$$

and for α_2 and α_3 when

$$\varepsilon_r = -3.85\varepsilon_m$$

where ε_r is the real part of ε. In turn, ε_r can be expressed according to Drude theory as

$$\varepsilon_r = 1 - \frac{{\omega_p}^2}{\omega^2 + \gamma^2}$$

where ω is the incident radiation frequency, γ is the loss-associated collision frequency term, and ω_p is the bulk plasma frequency, which is dependent on the density of free carriers in the nanodisk. Because both LSPR modes are generated at the same free-carrier concentration, ω_p must be equivalent for the two resonance conditions at the corresponding resonance frequencies, ω_{sp}. Inputting the experimental data from Figure 1 (where $\omega_{sp1} = 0.68$ eV, $\gamma_1 = 0.42$ eV, $\omega_{sp2} = 0.40$ eV, and $\gamma_2 = 0.06$ eV), we find that the short-wavelength LSPR band at $\lambda \approx 1800$ nm corresponds to the out-of-plane dipole and the long-wavelength LSPR band at $\lambda \approx 3100$ nm corresponds to the in-plane dipole. The value for ω_p is calculated to be in the range 1.25−1.29 eV, with the free-carrier density estimated as $(0.92-0.97) \times 10^{21}$ cm^{-3}. This is consistent with previously reported carrier densities for doped copper chalcogenides.[10,13]

Figure 2a displays the NIR extinction spectra for nanodisks with various aspect ratios. Nanodisks were grown by changing the reaction time for the thermal decomposition process, with the longest decomposition time of 60 min yielding an aspect ratio of 6.78 (Figure 2b). We observed that as the aspect ratio of the nanodisk increased, the LSPR wavelengths for both absorbance peaks blue-shifted to shorter wavelengths. These results differ from the behavior of shape-dependent LSPRs for anisotropic nanoparticles composed of noble metals such as Au or Ag. For example, Ag disks synthesized using colloidal methods are known to exhibit multiple intense scattering peaks in the optical range that are also due to the excitation of in-plane and out-of-plane dipolar LSPRs.[6,17,18] However, in studies where the aspect ratio of these metal nanodisks is systematically varied, the in-plane LSPR wavelength is expected to red-shift with increasing disk diameter, while the out-of-plane LSPR is expected to blue-shift. In contrast, both the in-plane and out-of-plane LSPR bands associated with the $Cu_{2-x}S$ nanodisks blue-shifted despite an almost 2-fold increase in aspect ratio.

For the $Cu_{2-x}S$ nanodisks, the observed blue-shifts in the LSPR wavelengths can be attributed to the sum of two effects: (1) an increase in nanodisk size and (2) an increase in the carrier density due to thermal oxidation, which has been suggested to form Cu vacancies in the chalcogenide lattice as a result of outward diffusion of Cu ions. Figure 2c shows the calculated shift

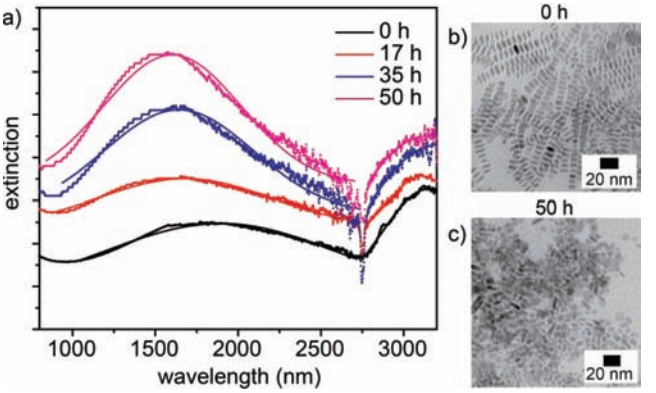

Figure 3. Change in LSPR properties with thermal treatment. (a) NIR extinction spectra of colloidal $Cu_{2-x}S$ nanodisk dispersions after various thermal treatment times, as shown. Corresponding TEM images of nanodisks (a) before and (b) after 50 h of treatment.

in the in-plane LSPR wavelength for each of these effects in comparison with the experimental data. Increasing the thermal decomposition time is expected to introduce a greater number of Cu vacancies into the lattice and thus to increase ω_{sp}, effectively counteracting the change in ω_{sp} expected from the increase in the nanodisk aspect ratio. This additive effect is consistent with the shift in LSPR wavelength of the out-of-plane mode, where the changes in shape and carrier concentration both contribute to a blue shift in the wavelength (see the SI). On the basis of the out-of-plane LSPR peak, the hole carrier density was observed to increase from $N_h = 0.80 \times 10^{21}$ cm^{-3} (for aspect ratio = 3.87) to $N_h = 1.21 \times 10^{21}$ cm^{-3} (for aspect ratio = 6.78). We also observed that the relative intensities of the two LSPR bands change significantly. A rapid rise in the peak intensity associated with the out-of-plane LSPR mode is attributed to the increase in total surface area of the basal plane per nanodisk. For plasmonic semiconductor nanocrystals, these results suggest that both shape effects and the effects of the free-carrier concentration must be carefully considered in tailoring the LSPR properties.

To study independently the effects of the carrier concentration on the shape-dependent LSPR modes of the nanodisks, we examined the effect of thermal treatment on nanodisks with the same aspect ratio. Figure 3 shows the changes in LSPR wavelength and intensity that accompany increasing thermal treatment times for a dispersion of $Cu_{2-x}S$ nanodisks with an aspect ratio of 3.87. Extended heating under ambient conditions would be expected to generate hole carriers in the $Cu_{2-x}S$ lattice as a result of oxidation. The spectra indicate that after 0, 17, 35, and 50 h of thermal treatment, the relative intensities of the in-plane and out-of-plane LSPR bands changed dramatically. The nanodisks did not undergo any shape or size change upon thermal treatment, as observed by TEM image analysis. Before treatment, the ratio of these intensities was 0.55, with the in-plane LSPR being dominant; after 50 h of treatment, the intensity ratio was 2.74, with the out-of-plane LSPR being dominant. Because the LSPR scattering and absorbance cross sections are directly related to the magnitude of the polarizability, the large enhancement of the out-of-plane LSPR suggests that charge localization occurs at the basal surfaces of the nanodisk as the hole-carrier concentration is increased. One possible explanation is that thermal treatment generates local surface charges as a result of dissociation or degradation of the dodecanethiol ligands that

dx.doi.org/10.1021/ja2089876 |J. Am. Chem. Soc. 2011, 133, 19072–19075

passivate the $Cu_{2-x}S$ surface. This is evidenced in the TEM images in Figure 3, which show dried colloidal droplets before and after thermal oxidation was carried out for 50 h. Before oxidation, the thiol-capped nanodisks preferred to assemble into long pancakelike stacks to minimize their surface energy. After thermal treatment, a similarly dried colloidal droplet did not display this tendency toward order, and the nanodisks remained segregated upon solvent evaporation. This suggests that the dodecanethiol ligands, which provide the strong hydrophobic driving force for nanodisk stacking, were no longer present. Another possible explanation for the change in relative LSPR peak intensity is that self-assembly into stacks causes the nanodisks to adopt an aligned orientation that favors the excitation of the in-plane LSPR mode. This is supported by XRD characterization showing enhancement of the (110) peak for powder samples prior to heat treatment (see the SI) Disassembly of the stacks then accounts for the increase in the intensity of the out-of-plane LSPR band. Future work will study the effects of self-assembly and capacitive coupling on the LSPR properties of anisotropic semiconductor nanocrystals.

Overall, these results demonstrate a commonality between the optical LSPR bands observed for anisotropic metallic nanoparticles and the NIR LSPR bands observed for semiconductor nanocrystals. They also show that shape tuning of semiconductor nanocrystals can access a large spectral range for LSPR excitation. Shape tuning may also provide a convenient strategy for subwavelength manipulation of electromagnetic radiation in the IR spectral region, with potential applications in thermal imaging and spectroscopy, IR-responsive coatings, and telecommunications.

■ ASSOCIATED CONTENT

Supporting Information. Detailed synthesis and methods section, XRD characterizations, calculation of the free-carrier density, and change in wavelength for the out-of-plane LSPR mode. This material is available free of charge via the Internet at http://pubs.acs.org.

■ AUTHOR INFORMATION

Corresponding Author
atao@ucsd.edu

■ ACKNOWLEDGMENT

Financial support was provided by NSF (ECCS-1125789). A.R.T. gratefully acknowledges support from a Hellman Fellowship. We thank the Kubiak Group at UCSD for use of their UV−vis−NIR spectrometer and Sabine Faulhaber and Norm Olson for their expertise.

■ REFERENCES

(1) Jin, R.; Cao, Y.; Mirkin, C. A.; Kelly, K. L.; Schatz, G. C.; Zheng, J. G. *Science* **2001**, *294*, 1901.
(2) Sherry, L. J.; Chang, S.-H.; Schatz, G. C.; Van Duyne, R. P.; Wiley, B. J.; Xia, Y. *Nano Lett.* **2005**, *5*, 2034.
(3) Link, S.; El-Sayed, M. A. *J. Phys. Chem. B* **1999**, *103*, 8410.
(4) Tao, A. R.; Habas, S.; Yang, P. *Small* **2008**, *4*, 310.
(5) Hutter, E.; Fendler, J. H. *Adv. Mater.* **2004**, *16*, 1685.
(6) Kelly, K. L.; Coronado, E.; Zhao, L. L.; Schatz, G. C. *J. Phys. Chem. B* **2003**, *107*, 668.
(7) Lal, S.; Link, S.; Halas, N. J. *Nat. Photonics* **2007**, *1*, 641.
(8) Anker, J. N.; Hall, W. P.; Lyandres, O.; Shah, N. C.; Zhao, J.; Van Duyne, R. P. *Nat. Mater.* **2008**, *7*, 442.
(9) Willets, K. A.; Van Duyne, R. P. *Annu. Rev. Phys. Chem.* **2007**, *58*, 267.
(10) Zhao, Y.; Pan, H.; Lou, Y.; Qiu, X.; Zhu, J.; Burda, C. *J. Am. Chem. Soc.* **2009**, *131*, 4253.
(11) Dorfs, D.; Härtling, T.; Miszta, K.; Bigall, N. C.; Kim, M. R.; Genovese, A.; Falqui, A.; Povia, M.; Manna, L. *J. Am. Chem. Soc.* **2011**, *133*, 11175.
(12) Garcia, G.; Buonsanti, R.; Runnerstrom, E. L.; Mendelsberg, R. J.; Llordes, A.; Anders, A.; Richardson, T. J.; Milliron, D. J. *Nano Lett.* **2011**, *11*, 4415.
(13) Luther, J. M.; Jain, P. K.; Ewers, T.; Alivisatos, A. P. *Nat. Mater.* **2011**, *10*, 361.
(14) Li, S.; Wang, H.; Xu, W.; Si, H.; Tao, X.; Lou, S.; Du, Z.; Li, L. S. *J. Colloid Interface Sci.* **2009**, *330*, 483.
(15) Larsen, T. H.; Sigman, M.; Ghezelbash, A.; Doty, R. C.; Korgel, B. A. *J. Am. Chem. Soc.* **2003**, *125*, 5638.
(16) Bohren, C. F.; Huffman, D. R. *Absorption and Scattering of Light by Small Particles*; Wiley: New York, 1998.
(17) Chen, S.; Fan, Z.; Carroll, D. L. *J. Phys. Chem. B* **2002**, *106*, 10777.
(18) Maillard, M.; Giorgio, S.; Pileni, M.-P. *J. Phys. Chem. B* **2003**, *107*, 2466.